Available online at www.sciencedirect.com
ScienceDirect
Journal of Molecular Catalysis A: Chemical 258 (2006) 346–354
JOURNAL OF MOLECULAR CATALYSIS A: CHEMICAL
www.elsevier.com/locate/molcata

Styrene epoxidation over cesium promoted silver nanowires catalysts

R.J. Chimentão [a], F. Medina [a,*], J.L.G. Fierro [b], J.E. Sueiras [a], Y. Cesteros [c], P. Salagre [c]

[a] *Dept. d'Enginyeria Química, Universitat Rovira i Virgili, 43007 Tarragona, Spain*
[b] *Instituto de Catalisis y Petroleoquimica, CSIC, Cantoblanco, 28049 Madrid, Spain*
[c] *Dept. de Química Inorgánica, Universitat Rovira i Virgili, 43005 Tarragona, Spain*

Received 28 June 2006; received in revised form 10 July 2006; accepted 11 July 2006
Available online 24 August 2006

Abstract

Epoxidation of styrene to styrene oxide (SO) by molecular oxygen was studied over cesium promoted silver nanowires catalysts. Styrene oxide (SO) and phenylacetaldehyde (Phe) were the main products. The results showed that Cs plays an important role improving the efficiency of the catalyst. The effect of the reaction temperature and the O_2:C_8H_8 molar ratio on the catalytic epoxidation was also investigated. Low reaction temperatures or high O_2:C_8H_8 ratios increase the selectivity to SO. The catalytic activity shows a maximum for silver nanowires promoted with 0.25 wt.% of Cs, achieving 94.6% of conversion and total selectivity to desired oxidation products (styrene oxide and phenylacetaldehyde). Besides, negligible deactivation of the catalyst was observed over 30 days of reaction. The experimental characterization was performed by X-ray diffraction (XRD), scanning electron microscopy (SEM), temperature-programmed reduction (TPR) and X-ray photoelectron spectroscopy (XPS). The presence of cesium plays a strong role in reducibility of the silver as detected by temperature-programmed reduction analysis affecting the catalytic activity. The results also suggested the presence of two different species of oxygen formed on the silver nanowires surface after oxygen exposure.

Keywords: Silver nanoparticles; Nanowires; Styrene; Cs; Epoxidation; XPS; SEM

1. Introduction

Direct gas phase partial oxidation of olefins by molecular oxygen to epoxides is long considered one of the most important reactions in commercial catalysis [1,2]. The styrene is a useful alkene model to study the mechanism reaction of terminal alkene epoxidation [3]. Silver is considered almost the unique effective catalyst for the heterogeneous epoxidation reaction [4]. In 1931, Lefort first reported success using silver as catalyst [5]. The ethylene epoxidation is the most studied partial oxidation reaction in industrial process and silver catalyst is the uniquely used under practical conditions [6].

It is well accepted that the selective oxidation reactions on supported noble metals catalyst proceed via Mars–van Krevelen mechanism. The redox property of the catalyst is therefore expected to play an important role in these reactions. Alkaline metals are observed to enhance the redox activities of a number supported metal catalysts [7]. Commercial catalysts for the epoxidation of ethylene consist of silver supported on low surface area materials such as α-Al_2O_3. Alkali metals and their salts have been proposed as promoters in these catalysts. Cesium is usually added to the catalyst to improve the selectivity toward the epoxide [8–13].

To understand the reaction mechanism, the adsorption of oxygen on silver catalysts has been thoroughly performed. This technique gives information about which type of adsorbed oxygen species are responsible in the epoxidation reaction. It has been observed that the oxygen shows different adsorption states. The studies devoted to oxygen-silver system suggests that mainly two different type of oxygen are the active species: electrophilic oxygen leading to selective oxidation products and nucleophilic oxygen producing combustion products [14]. These oxygen species exist on silver catalysts under ethylene epoxidation conditions (160–300 °C) through reversibly and irreversibly adsorption process. However, the study of oxygen adsorption on practical silver catalysts is especially complex since silver surfaces are polycrystalline and contains a significant proportion of defect [15]. Some results indicate that the (1 1 1) orientation is

* Corresponding author. Tel.: +34 977559787; fax: +34 977559667.
E-mail address: francesc.medina@urv.cat (F. Medina).

1381-1169/$ – see front matter © 2006 Elsevier B.V. All rights reserved.
doi:10.1016/j.molcata.2006.07.028

an important crystal face for real silver catalyst presumably due to the fact that it has the lowest surface energy [16]. There is a growing interest to obtain advanced materials using nanoscale building blocks, in order to control the sizes and shapes of inorganic nanocrystals [17,18]. Therefore the synthesis of well-controlled shapes of metal nanoparticles represents a new avenue in the study of selective oxidation reactions over silver catalysts.

Here an important objective of this work is to study how the size and morphology of silver nanoparticles affect the catalytic behavior of silver catalysts supported on α-Al_2O_3 in the selective oxidation of styrene in gas phase. Herewith we also investigated the performance of cesium promoted silver nanoparticles catalysts supported α-Al_2O_3 in the epoxidation of styrene. Styrene ($C_6H_5CH{=}CH_2$) is a good choice because the phenyl group π-electrons activate the olefinic bound towards electrophilic attack by oxygen [19]. In this work, silver nanowires were synthesized by polyol process [18] and then supported on α-Al_2O_3. Besides, the effect of the addition of cesium and the O_2:styrene molar ratios in the catalytic behavior were also studied. For comparison it was also studied a catalyst prepared by wetness impregnation with an aqueous solution of $AgNO_3$. Temperature-programmed reduction (TPR) and X-ray photoelectron spectroscopy (XPS) were performed to characterize the oxygen species formed on the silver nanowires after exposure to O_2. The samples were also structurally characterized using X-ray diffraction (XRD) and scanning electron microscopy (SEM), in order to correlate the morphological dependence of metal particles with its catalytic activity.

2. Experimental

2.1. Preparation of the catalysts

Silver nanowires catalysts were prepared by polyol process. In a typical synthesis of silver nanoparticles, 30 ml ethylene glycol solution of $AgNO_3$ (0.25 M, Aldrich) and 30 ml ethylene glycol solution of polyvinyl-pyrrolidone (PVP) (0.375 M in repeating unit weight-average molecular weight ≈40,000, Aldrich) were simultaneously added in 50 ml ethylene glycol at 433 K under vigorous magnetic stirring. The reaction mixture was then refluxed for 45 min at this temperature. The obtained nanoparticles were diluted with acetone and separated from ethylene glycol by centrifugation at 4000 rpm for 20 min. Then, silver nanowires (11 wt.%) were dispersed by impregnation on α-Al_2O_3 with an acetone solution. The α-Al_2O_3 support, that shows a surface area of around 0.4 m^2/g, was calcined at 673 K for 4 h before its use. For comparison, a silver catalyst obtained by support impregnation with an aqueous solution of silver nitrate with the same metal content (11 wt.%) was also prepared.

The procedure for catalyst activation, before the characterization and the activity tests, involved heating up to a temperature of 623 K in O_2 flow (heating rate 2 K/min), and then reduced in H_2 flow up to a temperature of 623 K (heating rate 5 K/min) at atmospheric pressure, followed by isothermal reduction at this temperature for 3 h. To investigate the promotion effect by cesium the catalysts were impregnated by an aqueous solution containing appropriate amounts of CsOH. After that the promoted catalyst was activated using the same protocol.

2.2. Catalyst characterization

2.2.1. X-ray diffraction (XRD)

XRD measurements were made using a Siemens D5000 diffractometer (Bragg–Bentano parafocusing geometry and vertical θ–θ goniometer) fitted with a curved graphite diffracted-beam monochromator, incident and diffracted-beam Soller slits, a 0.06° receiving slit and scintillation counter as detector. The angular 2θ diffraction range was between 30° and 120°. The data were collected with an angular step of 0.05° at 3 s per step and sample rotation. Cu K_α radiation was obtained from copper X-ray tube operated at 40 kV and 30 mA.

2.2.2. Scanning electron microscopy (SEM)

The morphologies of the catalysts were observed by SEM with a JEOL JSM-35C scanning microscope operated at an acceleration voltage of 15 kV. A small portion of each sample powder was coated on a metallic disk holder and covered with a thin gold layer before the SEM analysis.

2.2.3. Temperature-programmed reduction (TPR)

TPR experiments were performed in a TPDRO 1100 (Thermo Finnigan), equipped with a thermal conductivity detector (TCD) and coupled to a mass spectrometer QMS 422 Omnistar. The catalysts were treated in O_2 for 1 h at 623 K before TPR analysis. Then, the samples were purged with argon flow before the TPR analysis. The TPR of silver catalysts was carried out using 5% H_2 in Ar flow as reducing agent, the gas flow rate was 20 ml/min and the weight of sample was 1.0 g. The gases evolved during the TPR experiment was monitored by TCD and mass spectrometer detector. The temperature was raised from 323 up to 1073 K at a rate of $\beta = 20$ K/min. Water produced during TPR was trapped in $CaO + Na_2O$ (soda lime).

2.2.4. X-ray photoelectron spectroscopy (XPS)

The XPS analyses were acquired in a VG Escalab 200R electron spectrometer equipped with a hemispherical electron analyzer operating in a constant pass energy mode and a non-monochromatic Mg Kα ($h\nu = 1253.6$ eV; $1\text{ eV} = 1.603 \times 10^{-19}$ J). X-ray source operated at 10 mA and 12 kV. Kinetic energies of photoelectrons were measured using a hemispherical electron analyzer working in the constant pass energy mode. The background pressure in the analysis chamber was kept below 7×10^{-9} mbar during data acquisition. The powder samples were pressed into copper holders and then mounted on a support rod placed in the pretreatment chamber. All the spectra were signal-averaged for at least 80 scans and were taken in increments of 0.1 eV with dwell times of 50 ms. The sample cleaning was performed by cycles of Ar^+ etching (1.5 keV, 5 min), oxygen treatments at 573 K with subsequent annealing in vacuum. After three cycles of cleaning carbon contamination was very low and the remaining C 1s signal was used to calibrate the binding energies (BE C 1s = 284.9 eV). High resolution spectral envelopes were obtained by curve fit-

ting synthetic peak components using the software XPS peak. Symmetric Gaussian–Lorentzian product functions were used to approximate the line shapes of the fitting components.

2.3. Catalytic activity

The catalytic epoxidation of styrene was performed in a stainless steel tubular down flow reactor. The size of the fix-bed reactor was Ø10 mm × 20 cm long provided with a temperature control system. Reaction temperature was measured in the middle of the catalyst bed by means of a K-type thermocouple. The reactor was filled with the catalyst (1.0 g), which had been previously ground and sieved in the range of 75–100 mesh. The reactor was placed in an electric furnace with a temperature control system. A pressure indicator was used to measure the pressure drop in the catalyst bed. Catalytic activity was measured at steady state conditions (after 5 h of time on stream). The feedstock gas, consisted of a mixture of O_2–Ar, was fed to the reactor by independent mass flow controllers, using a total flow rate between 100 and 300 ml/min. The styrene was introduced into the reactor by a high-pressure metering pump, which worked in a flow-rate range of 0.1–1.0 ml/h. The reaction temperatures were in the range of 503–623 K working at atmospheric pressure. The effluent gas was rapidly cooled and analyzed off-line using a Shimadzu GC 2010 gas-chromatograph equipped with an Ultra 2 capillary column and flame ionization detector (FID). The presence of combustion products was determined by on-line TCD and mass spectrometer.

3. Results and discussion

3.1. Silver nanowires catalysts characterization

X-ray diffraction (XRD) pattern of the nanowires synthesized by the polyol process suggested that silver existed purely in the face-centered cubic (fcc) structure ((a) in Fig. 1(A)). The diffraction pattern of the silver nanowires did not suggest the presence of possible impurities such as Ag_2O and $AgNO_3$. The peaks detected for the silver nanoparticles were assigned to diffraction from the (1 1 1), (2 0 0) and (2 2 0) planes. The lattice constant calculated by XRD for the silver nanowires was 4.0839 Å, which is very close to the report data ($a = 4.0862$ Å, joint committee on powder diffraction standards file 04-0783). The ratio of intensity between (1 1 1) and (2 0 0) diffraction lines for silver nanowires was higher than for the file JCPDS (4.5 versus 2.5) for the standard silver ((b) in Fig. 1(A)) indicating that the nanowires show preferred orientation in (1 1 1) facets. This fact indicates that silver nanowires tend to grow as bicrystals twinned along the (1 1 1) planes, showing (1 1 1) crystal faces at their surface [20]. Twinning is the mechanism for forming these particles and it is the result of two subgrains sharing a common crystallographic plane [21]. Fig. 1(B) shows the XRD patterns of the 11% $Ag^{(0.25\%\ Cs\text{-}NW)}/\alpha\text{-}Al_2O_3$ fresh and after 30 days of reaction catalysts. XRD only revealed the presence of metallic Ag not detecting the presence of silver oxide peaks. Besides, the presence of Cs was not detected probably due to the low amount. It is important to mention that the XRD pattern for both catalysts

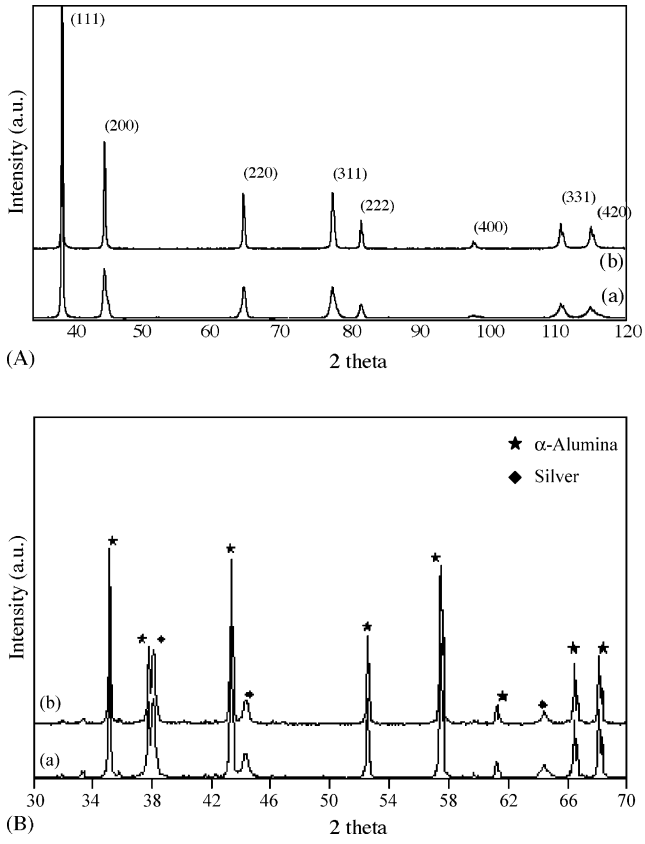

Fig. 1. (A) XRD of the silver nanowires (a) and standard silver sample (b). (B) Pattern obtained for the 11% $Ag^{(NW\text{-}0.25\%\ Cs)}/\alpha\text{-}Al_2O_3$ catalyst: (a) fresh; (b) after 30 days on stream.

is quite similar. This indicates that after a period of reaction of 30 days the particle size and the morphological structure of the catalyst were preserved.

Fig. 2(a) shows the SEM image of the silver catalyst obtained by impregnation with an aqueous solution of silver nitrate. SEM image shows the presence of irregular Ag particles distributed on the $\alpha\text{-}Al_2O_3$ support. However, the SEM image observed in Fig. 2(b) shows a well dispersion of silver nanowires on the support. The diameters of these nanowires were reasonable uniform, with an average value of 150 nm. Together with the silver nanowires (but in low amount) the presence of nanocubes and nanopolyhedra were also observed. The cross section of the Ag nanowires (inset Fig. 2(b)) clearly presents a pentagonal shape according to previous studies [22,23].

TPR analysis was used to characterize the oxygen species formed by exposure of silver catalyst under O_2 flow. Prior to the TPR experiments, catalyst samples were treated in oxygen at 623 K. Fig. 3(1–5) shows the TPR profiles of the silver nanowires with different loading of cesium. The unpromoted silver nanowires catalyst (11% $Ag^{(NW)}/\alpha\text{-}Al_2O_3$) and the silver impregnated catalyst (11% $Ag/\alpha\text{-}Al_2O_3$) are also shown in the inset of Fig. 3.

The peaks observed in TPR can be assigned based on the temperature at which they appear. Previous studies have shown that the peak around 600 K is attributed to the presence of subsurface oxygen (O_β) [24–30]. Furthermore, the presence of reduction

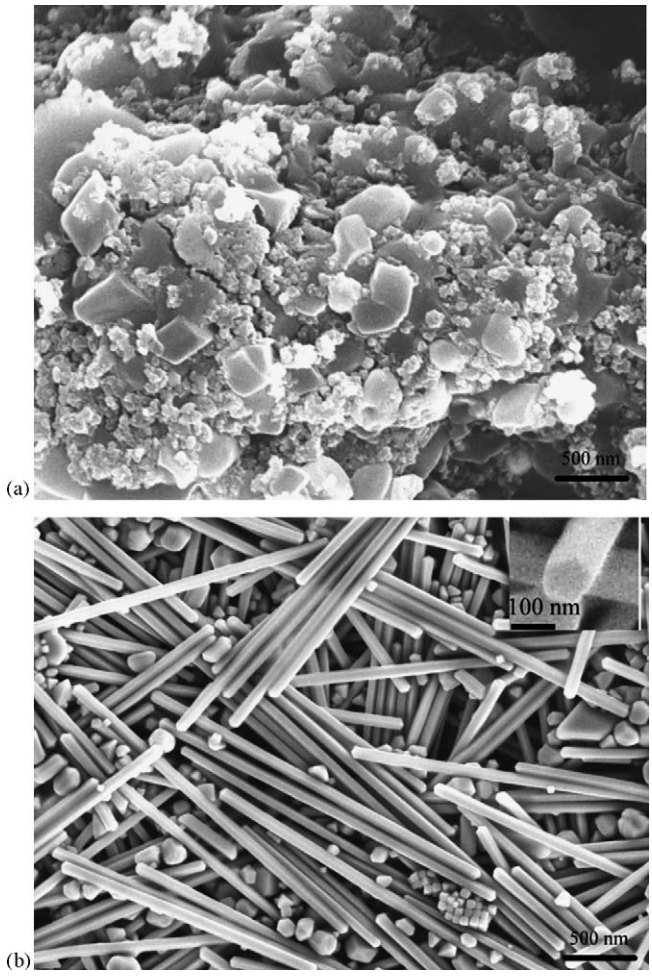

Fig. 2. SEM image of silver impregnated catalyst (a), and silver nanowires catalyst (b).

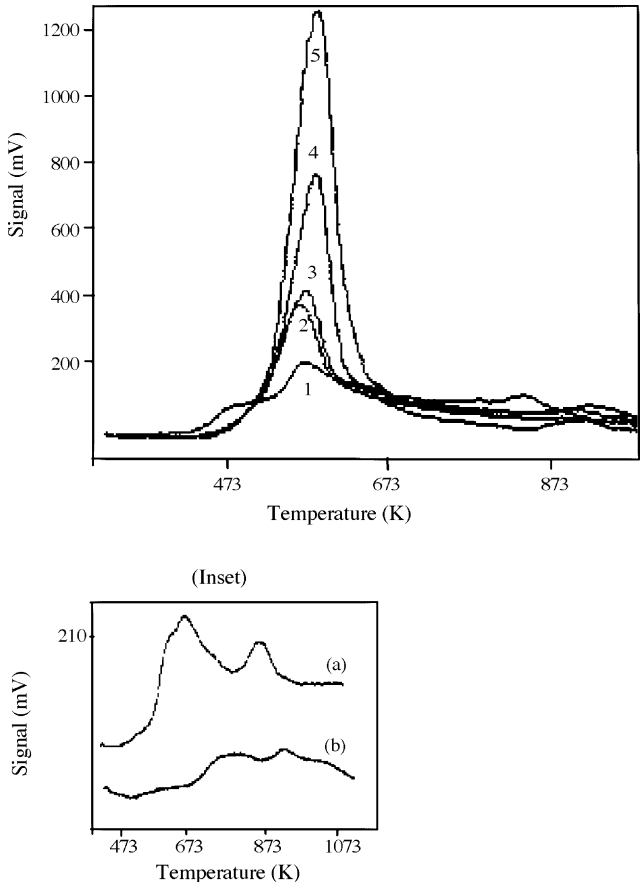

Fig. 3. Temperature-programmed reduction profiles of silver catalysts with different loading of cesium (referred to the silver content): (1) 0.0625%, (2) 0.125%, (3) 0.25%, (4) 0.5%, and (5) 1.0%. Inset: (a) unpromoted silver nanowires; (b) silver impregnated catalyst.

peaks at higher temperatures can be attributed to the presence of oxygen species that are strongly chemisorbed on the surface of silver and are labeled as (O_γ) [27,31–34].

TPR results show that the impregnated catalyst has the lowest intense reduction peaks when compare with silver nanowires ones. Besides, the reduction peaks appear at higher temperatures (753 and 933 K) (see the inset (b) of Fig. 3). The most intense peak for this catalyst is the second one. However, more intense reduction peaks are observed for silver nanowires catalyst. The unpromoted silver nanowires catalyst (inset (a) of Fig. 3) shows two broad peaks at around 623 K (the most intense peak) and 873 K. So, the main oxygen species for this catalyst is the O_β. When silver nanowires were promoted by Cs a strong increase in the signal of the first peak of TPR was observed. It is noteworthy to observe that T_{max} value first decreased when the pure silver nanowires were promoted with 0.0625 wt.% of cesium content and then shifted toward higher values when the cesium content continues increasing. However, the reduction peaks (T_{max}) for cesium promoted catalysts are always shifted to lower temperatures in comparison with unpromoted silver ones. Table 1 shows the temperature of peak maxima and the hydrogen consumption of this first peak at different cesium amount. The signal increased with cesium loading. Furthermore, for Cs promoted catalysts a broad peak at higher reduction temperature (between 700 and 950 K) with very low intensity was also observed. This indicates the presence of O_γ on the surface of the silver particles even at these higher reduction temperatures.

The analysis of the near surface of the silver nanowires was performed by XPS technique. The study of the electronic state by XPS was carried out on non supported silver nanowires in order to avoid the overshadowed of the oxygen component arising from the α-Al_2O_3 support. However the presence of oxygen component arising from the promoter (cesium oxide) is expected. The XPS profiles of the unpromoted and cesium promoted silver nanowires are depicted in Fig. 4(A) and (B), respectively. Table 2 shows the binding energies values for unpromoted silver nanowires and 0.25 wt.% cesium promoted silver nanowires samples oxidized at 623 K and reduced in situ in the XPS equipment between 573 and 773 K.

Fig. 4(A) shows the XPS spectra of the oxidized silver nanowires (a) and then reduced at 573, 673, and 773 K ((b), (c), and (d), respectively). The XPS profile of the unpromoted silver nanowires (Fig. 4(A)) showed only one peak for the binding energy of Ag $3d_{5/2}$ centered between 367.5 and 367.7 eV as is shown in Table 2 that can be ascribed to Ag_2O [34]. This is

Table 1
Results of temperature-programmed reduction and catalytic activity at 523 K

Catalyst	TPR analysis		Catalytic activity tests		
	T_{max} (K)	H_2 consumption (μmol/g)[a]	X (%)[b]	Phe (%)[c]	SO (%)[d]
11% Ag/α-Al_2O_3	753	0.5	1.0	51.4	48.6
11% $Ag^{(NW)}$/α-Al_2O_3	623	1.3	10.0	57.5	42.5
11% $Ag^{(NW\text{-}0.0625\%\ Cs)}$/α-$Al_2O_3$	568	2.6	50.9	48.6	51.4
11% $Ag^{(NW\text{-}0.125\%\ Cs)}$/α-$Al_2O_3$	570	2.7	60.1	46.8	53.2
11% $Ag^{(NW\text{-}0.25\%\ Cs)}$/α-$Al_2O_3$	572	2.8	94.6	44.4	55.6
11% $Ag^{(NW\text{-}0.30\%\ Cs)}$/α-$Al_2O_3$	575	3.8	90.5	26.7	73.3
11% $Ag^{(NW\text{-}0.5\%\ Cs)}$/α-$Al_2O_3$	583	4.9	72.4	25.1	74.9
11% $Ag^{(NW\text{-}1.0\%\ Cs)}$/α-$Al_2O_3$	587	8.1	42.3	24.1	75.9

[a] Peak signal from the first peak detected by temperature-programmed reduction (TPR).
[b] Conversion (X).
[c] Selectivity to phenylacetaldehyde (Phe%).
[d] Selectivity to styrene oxide (SO%), O_2:C_8H_8 molar ratio of 50.

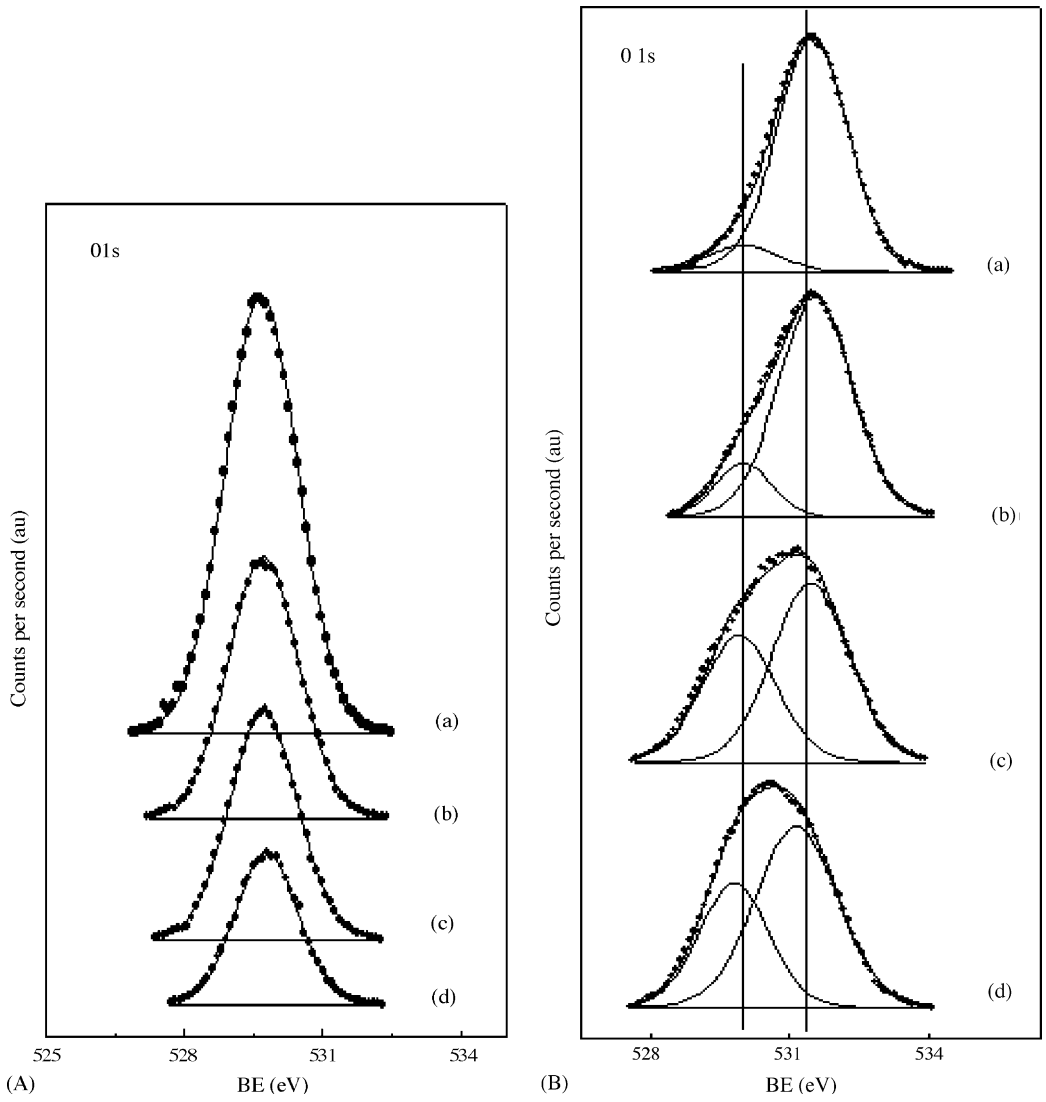

Fig. 4. XPS profiles of the silver nanowires (A) and promoted by 0.25% of Cs (B) after oxidation at 623 K (a), and then reduced at different temperatures: (b) 573 K; (c) 673 K; (d) 773 K.

Table 2
Binding energies (eV) and surface atomic ratios of silver nanowires

Treatment	Binding energy (eV), Ag nanowires		Binding energy (eV), 0.25% Cs promoted Ag nanowires		
	Ag $3d_{5/2}$	O 1s	Ag $3d_{5/2}$	O 1s	Cs $3d_{5/2}$
Oxidation at 623 K	367.6	529.7	367.7	529.9 (10); 531.5 (90)	724.0
Reduction at 573 K	367.7	529.7	367.7	529.9 (16); 531.6 (84)	723.9
Reduction at 673 K	367.6	529.7	367.4	529.8 (39); 531.4 (61)	723.9
Reduction at 773 K	367.5	529.8	367.5	529.8 (40); 531.2 (60)	724.1

also confirmed by the value of O/Ag of around 0.48 obtained by XPS for the unpromoted oxidized sample. Besides, the binding energy values are around of 367.5 eV for samples reduced at 773 K. This indicates that under reduction conditions, in the XPS equipment, the first atomic layers of the surface of silver nanowires (that have the main contribution to the XPS signal) are in oxidized state. This fact indicates the presence of oxygen species with a strong interaction with the silver surface (O_γ), which are difficult to reduce even at 773 K, in agreement with TPR results. From Table 2, the O 1s peak signal observed for the unpromoted silver nanowires was around 529.7 eV for both reduced and oxidized samples. However, when cesium was added (Fig. 4(B)), the O 1s peak showed two components, the major one at around 531.5 eV and a less intense one at around 529.8 eV. These O-species have been ascribed to O_β and O_γ species respectively [25,31]. The distinction between different types of oxygen detected by XPS was recognized on the basis of the way in which of the oxygen specie was embedded into the surface lattice of the silver nanowires. From the XPS spectra of the unpromoted silver nanowires the O_γ was the unique specie detected on the surface of the nanowires. When 0.25 wt.% of cesium was introduced on the silver nanowires the O_β was the major oxygen species detected by XPS as shown in Table 2. It seems that the addition of Cs promotes the formation of the O_β species. Fig. 4(B) also shows the XPS spectra of the oxidized sample (a) and reduced at 573, 673, and 773 K ((b), (c), and (d), respectively). The deconvoluted peak of the O 1s component with a binding energy value of around 531.5 eV represents around 90% for the cesium promoted silver nanowires oxidized at 623 K. Further information about the nature of oxygen species on the cesium promoted silver nanowires surface was obtained by monitoring the reduction of the nanowires under hydrogen during XPS analysis. From Fig. 4(B), the O 1s component at around 531.5 eV of the Cs promoted silver nanowires sample decreases its relative intensity from 90 to 60% as the reduction temperature increases. In parallel, the O 1s component at around 529.8 eV increases its relative intensity from 10 to 40%. The increase in the relative signal of this O 1s component can be attributed to the decrease in the signal of the peak around 531.5 eV due to the reduction process, as well as the formation of new O_γ species probably by interstitial diffusion of the subsurface oxygen (O_β) to the catalyst surface [31]. The presence of the peak around 531.5 eV at higher reduction temperature (773 K) could be also attributed to the contribution of the oxygen of cesium oxide species [35], which is overlapping the peak of the O_β species.

3.2. Catalytic activity

The selective oxidation of styrene, at steady state, over silver catalysts shows phenylacetaldehyde (Phe) and styrene oxide (SO) as the main products. Table 1 shows the catalytic performance of the silver catalysts for the epoxidation of styrene with molecular oxygen as oxidant at a reaction temperature of 523 K. A blank test run with the α-Al_2O_3 support showed no conversion of styrene at the reaction temperatures studied. Silver impregnated catalyst showed a styrene conversion of 1.0% at 523 K. However, a conversion of 10% and selectivity to styrene oxide of 42.5% was observed at the same reaction conditions for silver nanowires catalyst. It is important to mention that the deactivation of the catalyst during an operation time of 30 days was negligible. The promotion of silver nanowires catalysts with cesium increased the catalytic activity up to 94.6% for a cesium loading of 0.25 wt.%. Besides, the selectivity to styrene oxide increased from 42.5 up to 75.9% when silver nanowires catalyst was promoted with 1 wt.% of cesium. In the case of catalytic oxidation reactions it is well accepted that the redox properties of the catalyst play a fundamental role on the activity [7,36]. Alkali metals are electropositive promoters, which act to enhance the chemisorption of electron acceptor adsorbates and weaken chemisorption of electron donor adsorbates, as they themselves are electron donors. Besides, the incorporation of an alkaline metal may result in a decrease in surface acidity, since acid sites are neutralized [37]. The enhancement in epoxide selectivity observed in the presence of CsOH was probably due to suppression of acid centers in the α-Al_2O_3 support and hence the isomerization route of styrene oxide to phenylacetaldehyde was decreased. Consequently, the addition of cesium increased both the catalytic activity and the selectivity to the epoxide. So, the cesium modified the Ag surface particularly toward the epoxidation direction. Previous experimental studies have show that some alkenes without allylic hydrogen atoms, such as ethylene, can be directly epoxidize with high selectivity with molecular oxygen in the gas phase over Ag catalysts [38]. In line with these studies, the catalytic results observed for our silver nanowires catalysts indicates that these materials are indeed very active for epoxidation since styrene has no allylic hydrogens. Thus it is really expected that the styrene behave as ethylene in epoxidation over the silver catalysts. Moreover previous studies [39] have also shown that this reaction is sensitive to particle size and more selective on large particles. This fact can also reinforce the high catalytic performance on the silver nanowires since these materials are dominated by dense crystal planes.

Table 3
ICP-AES and XPS surface analysis of silver nanowires catalyst

Catalyst	ICP-AES analysis (atomic ratio)		XPS analysis (atomic ratio)	
	Cs/Al	Cs/Ag	Cs/Al	Cs/Ag
11% $Ag^{(NW\text{-}0.125\%\ Cs)}/\alpha\text{-}Al_2O_3$	0.00005	0.0009	0.005	0.119
11% $Ag^{(NW\text{-}0.25\%\ Cs)}/\alpha\text{-}Al_2O_3$	0.0001	0.0018	0.009	0.240
11% $Ag^{(NW\text{-}0.5\%\ Cs)}/\alpha\text{-}Al_2O_3$	0.0002	0.0036	0.020	0.119
11% $Ag^{(NW\text{-}1.0\%\ Cs)}/\alpha\text{-}Al_2O_3$	0.0004	0.0072	0.023	0.220

The silver nanowires catalyst promoted by 0.25 wt.% of Cs showed the highest conversion of 94.6% for the styrene. The fact that both activity and selectivity change with the amount of Cs on Ag catalysts strongly suggests that the promotion effect is electronic in origin [40]. However, the activity increases up to a cesium loading of 0.25 wt.% and beyond this amount the conversion of styrene decreases progressively. The decrease of conversion at higher Cs loadings (Cs > 0.25 wt.%) can be probably attributed to the effect of cesium dispersion. The excess of cesium can block the active surface and thus decrease the catalytic activity. This change in the catalytic activity is also intimately correlated with results obtained by XPS depicted in Table 3. On the basis of the XPS results in Table 3 the sample with a cesium loading of 0.125 wt.% shows a Cs/Ag atomic ratio of 0.119. When the cesium increased up to 0.25 wt.% the Cs/Ag ratio increased up to 0.24. This proportion between Cs/Ag ratio and the amount of Cs in the sample indicates that cesium is well dispersed on the surface of silver nanowires. However for samples with higher cesium content the Cs/Ag atomic ratios decreased. For instance, the 11% $Ag^{(NW\text{-}0.5\%\ Cs)}/\alpha\text{-}Al_2O_3$ sample, which has two times of cesium amount than for 11% $Ag^{(NW\text{-}0.25\%\ Cs)}/\alpha\text{-}Al_2O_3$, the Cs/Ag molar ratio detected by XPS analysis is lower (0.119). Similar behaviour is observed for the catalysts with a cesium amount of 1.0 wt.% that shows a Cs/Ag ratio quite similar than for the catalyst with a cesium amount of 0.125 wt.%. This indicates that agglomeration of cesium species on the silver surface is produced at higher cesium loading that covers the silver surface producing the poisoning of the active sites. Thus, the increase in the cesium content may cover progressively the silver surface decreasing the active sites.

Furthermore, correlating the epoxidation performance with the XPS results, it was also found that there is a direct relationship between the epoxidation performance of catalyst and O1s signal associated with O_β specie. The O_β species seems to be critical for the activation of the silver for this reaction. This can also explain both the low activity and selectivity observed for the 11% $Ag/\alpha\text{-}Al_2O_3$ impregnated catalyst since the main oxygen species detected is O_γ that is more strongly bound and harder to react. There is a strong correlation between the peak signal of the O_β specie with the catalytic activity toward the epoxidation of the styrene. This specie seems to be responsible for the high activity and selectivity while the strongly adsorbed surface atomic oxygen (O_γ) showed lower activity.

In line with these observations, the shift of peak maxima (T_{max}) in the TPR analysis (Table 1) to lower temperatures for the cesium promoted silver nanowires samples may clearly indicate the formation of more reducible silver species compared with the unpromoted samples. All the cesium promoted samples presented higher catalytic activity compared to the unpromoted silver samples (pure silver nanowires (11% $Ag^{(NW)}/\alpha\text{-}Al_2O_3$) and impregnated sample (11% $Ag/\alpha\text{-}Al_2O_3$)) which could be a consequence of electronic effects of the cesium on the properties of the silver since alkaline metals may act as electron donator [37] increasing the electron density of Ag and hence affecting their reducibility. When the silver nanowires were promoted by 0.25 wt.% of cesium the conversion of styrene and the selectivity to styrene oxide increased. However, with higher cesium content (Cs > 0.25 wt.%) the styrene conversion decreased. This fact is also reinforced by the XPS results depicted in Table 3. At higher Cs content (>0.25 wt.%) the active silver surface are been probably disengaged from the catalytic cycle by Cs, however those still active do not suffer from any modification by cesium and this maybe the reason that the selectivity remains unaffected. In fact since repetitive redox cycles occur during the selective oxidation of styrene it also can be suggested that the low catalytic activity observed for the unpromoted silver samples may be due to the fact that the oxidation–reduction cycle is more difficult than for the cesium promoted silver nanowires samples. So, cesium promotion may play an important role increasing the catalytic activity as well as preventing the isomerization route to phenylacetaldehyde.

Table 4 lists the conversion and selectivity to styrene oxide on 11% $Ag^{(NW\text{-}0.25\%\ Cs)}/\alpha\text{-}Al_2O_3$ catalyst at 503 K with different C_8H_8:O_2 molar ratios. The increase in the O_2:C_8H_8 molar ratio improved the conversion and selectivity to styrene oxide. When the O_2:C_8H_8 molar ratio was 25, the conversion was 59.3% and the selectivity reaches 55.3%, while for O_2:C_8H_8 molar ratio of 150 the conversion was 84.2% and the selectivity to styrene oxide was 73.5%. These results are in agreement with previous results [38]. It seems that an oxygen rich atmosphere is also beneficial for both activity and selectivity in the epoxidation reaction of styrene. This fact indicates a strong competition between styrene and oxygen on the active sites of the catalyst.

Fig. 5 shows the catalytic behaviour of cesium promoted silver nanowires catalysts at different reaction temperatures, such as 503, 513, and 523 K. The results show that the amount of cesium in the catalyst plays an important role in the conversion in the range of the temperatures studied. Catalyst containing 0.25 wt.% of cesium showed the highest activity in all the range of temperatures reaction tested the styrene conversion over silver nanowires catalysts changes with the cesium loading. Higher reaction temperature improves the catalytic activity but reduces the selectivity to SO. At 503 K, the selectivity to SO was 68.4%

Table 4
Conversion and selectivity at different O_2:C_8H_8 molar ratios for styrene epoxidation reaction on 11% $Ag^{(NW\text{-}0.25\%\ Cs)}/\alpha\text{-}Al_2O_3$ catalyst[a]

Molar ratio, O_2:C_8H_8	Conversion (%)	Selectivity to SO (%)
25	59.3	55.3
50	76.5	68.4
100	79.7	70.5
150	84.2	73.5

[a] Reaction temperature, 503 K.

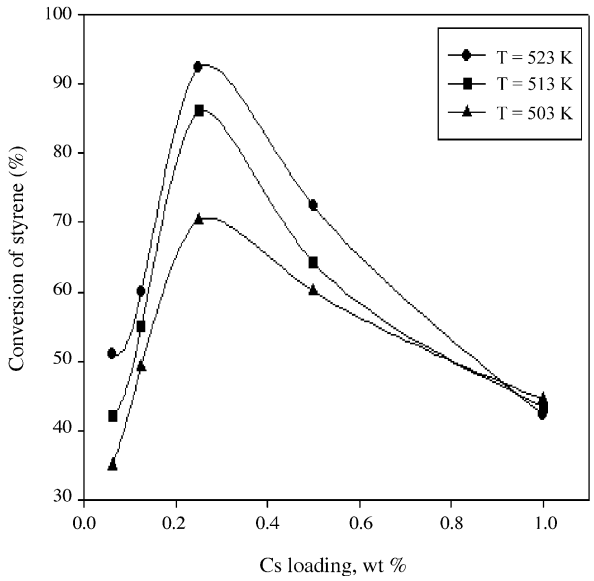

Fig. 5. Catalytic activity of cesium promoted silver nanowires catalysts at different reaction temperatures.

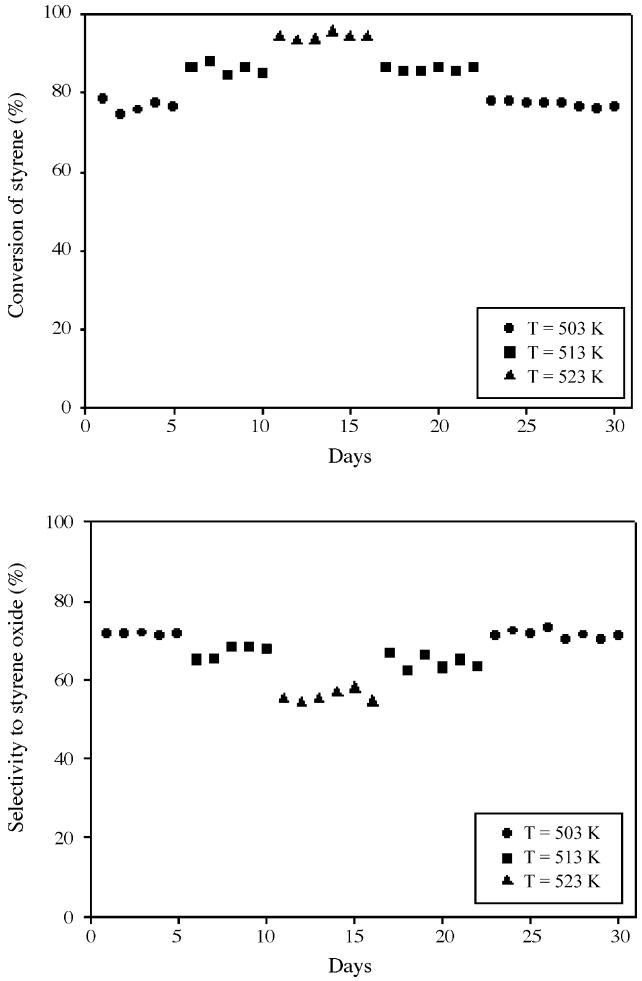

Fig. 6. Catalytic activity of 11% $Ag^{(NW\text{-}0.25\%\ Cs)}/\alpha\text{-}Al_2O_3$ catalyst in the epoxidation of styrene as a function of time on stream and reaction temperature.

and the styrene conversion was 76.5%. At 523 K the selectivity to SO decreased to 55.6% while the conversion of styrene increased to 94.6%.

In order to study the stability of the catalysts, a reaction test during a period of 30 days was performed using the silver nanowires catalyst containing 0.25 wt.% of cesium. The activity and selectivity at different reaction temperatures (503, 513, and 523 K), and an O_2:C_8H_8 molar ratio of 100, are shown in Fig. 6 as a function of time on stream. As the reactor temperature was increased the selectivity to the epoxide decreased. A styrene conversion of around 79% and selectivity to styrene oxide of around 70% was achieved during the first five days of reaction at 503 K. Then, the reaction was carried out at 513 K on the following five days and the conversion of styrene increased up to 86.2% while the selectivity to SO decreased to 66.6%. After 10 days of reaction the temperature was increase from 513 to 523 K and the conversion of styrene increased up to 94.6% while the selectivity to SO decreased to 55%. This cycle was repeated again obtaining similar catalytic behaviour. This indicates that this catalyst was stable during this reaction test.

4. Conclusions

Styrene epoxidation by oxygen was carried out on silver nanowires promoted with different contents of cesium. Addition of CsOH significantly improves conversion of styrene and the selectivity to SO. The maximum activity was obtained when the silver nanowires were promoted by 0.25% of Cs. A higher reaction temperature can improve the activity of the catalyst, but reduces the selectivity to SO. TPR experiments indicated that the cesium affected the reducibility of the silver. Besides, the selectivity to styrene oxide was enhanced by cesium promotion. The selectivity to styrene oxide was also enhanced in oxygen rich atmosphere. Furthermore, correlating the epoxidation performance with the XPS results, can be stated that there is a direct relationship between the epoxidation performance of catalyst and O 1s signal associated with O_β specie. The O_β species seems to be critical for the activity of the silver catalysts. Besides, negligible deactivation of the silver nanowires catalyst promoted with 0.25% of cesium was observed over 30 days of reaction. These results indicate the feasibility of shape controlled silver nanoparticles as catalysts for styrene epoxidation and how the activity and selectivity of the catalyst can be changed by Cs promotion.

Acknowledgements

This work was supported by the Ministerio de Ciencia y Tecnologia (Spain) under projects REN2002-04464-CO2-01 and PETRI 95-0801.OP. Thanks are also due to Destilaciones Bordas SA.

References

[1] A.K. Santra, J.J. Cowell, R.M. Lambert, Catal. Lett. 67 (2000) 87.
[2] T.S. Ahmadi, Z.L. Wang, T.C. Green, A. Henglein, M.A. El-Sayed, Science 272 (1996) 1924.

[3] R.B. Grant, R.M. Lambert, J. Catal. 93 (1985) 92.
[4] C.T. Campbell, J. Phys. Chem. 89 (1985) 5789.
[5] T.E. Lefort, Fr. Pat. 729,952 (March 27, 1931) (to Societe Francaise de Catalyse Generalise), and subsequent additions.
[6] W.M.H. Sachtler, C. Backx, R.A. Van Santen, Catal. Rev. Sci. Eng. 23 (1–2) (1981) 127.
[7] J. Haber, in: G. Ertl, H. Knozinger, J. Weitkamp (Eds.), Handbook of Heterogeneous Catalysis, vol. 5, VCH, Weinheim, 1997, p. 2253.
[8] W.S. Epling, G.B. Hoflund, D.M. Minahan, J. Catal. 171 (1997) 490.
[9] N. Macleod, J.M. Keel, R.M. Lambert, Catal. Lett. 86 (2003) 51.
[10] E.A. Podgornov, I.P. Prosvirin, V.I. Bukhtiyarov, J. Mol. Catal. A: Chem. 158 (2000) 337.
[11] J.R. Monnier, J.L. Stavinoha Jr., R.L. Minga, J. Catal. 226 (2004) 401.
[12] C.T. Campbell, B.E. Koel, J. Catal. 92 (1985) 272.
[13] J.J. Cowell, A.K. Santra, R. Lindsay, R.M. Lambert, A. Baraldi, A. Goldini, Surf. Sci. 437 (1999) 1.
[14] E.A. Carter, W.A. Goddard III, Surf. Sci. 209 (1989) 243.
[15] G.I.N. Waterhouse, G.A. Bowmaker, J.B. Metson, Appl. Surf. Sci. 214 (2003) 36.
[16] X. Bao, M. Muhler, B. Pettinger, R. Schlögl, G. Ertl, Catal. Lett. 22 (1993) 215.
[17] V.F. Puntes, K.M. Krishnan, A.P. Alivisatos, Science 291 (2001) 2117.
[18] Y. Sun, Y. Xia, Science 298 (2002) 2176.
[19] F.J. Williams, D.P.C. Bird, E.C.H. Sykes, A.K. Santra, R.M. Lambert, J. Phys. Chem. B 107 (2003) 3824.
[20] B.D. Cullity, S.R. Stock, Elements of X-Ray Diffraction, 2nd ed., Prentice Hall, New Jersey, 2001.
[21] Z.L. Wang, J. Phys. Chem. B 104 (2000) 1153.
[22] Y. Gao, P. Jiang, D.F. Liu, H.J. Yuan, X.Q. Yan, Z.P. Zhou, J.X. Wang, L. Song, L.F. Liu, W.Y. Zhou, G. Wang, C.Y. Wang, S.S. Xie, Chem. Phys. Lett. 380 (2003) 146.
[23] M.R. Salazar, J.D. Kress, A. Redondo, Surf. Sci. 469 (2000) 80.
[24] A.J. Nagy, G. Mestl, D. Herein, G. Weinberg, E. Kitzelmann, R. Schlögl, J. Catal. 182 (1999) 417.
[25] A.J. Nagy, G. Mestl, Appl. Catal. 188 (1999) 337.
[26] A.J. Nagy, G. Mestl, R. Schlögl, J. Catal. 188 (1998) 58.
[27] D. Herein, A. Nagy, H. Schubert, G. Weinberg, E. Kitzelmann, R. Schlögl, Z. Phys. Chem. 197 (1996) 67.
[28] G.I.N. Waterhouse, G.A. Bowmaker, J.B. Metson, Appl. Catal. 265 (2004) 85.
[29] G.A. Somorjai, Introduction to Surface Chemistry and Catalysis, Wiley, New York, 1994.
[30] W.X. Li, C.S. Stampfl, M. Scheffler, Phys. Rev. B 67 (2003) 045408.
[31] X. Bao, M. Muhler, T. Scedel-Niedrig, R. Schlögl, Phys. Rev. B 54 (1996) 2249.
[32] A. Nagy, G. Mestl, T. Rüle, G. Weinberg, R. Schlögl, J. Catal. 179 (1998) 548.
[33] G.I.N. Waterhouse, G.A. Bowmaker, J.B. Metson, Appl. Catal. 266 (2004) 257.
[34] XPS International Fundamental XPS Data Tables, available at: http://www.xpsdata.com.
[35] C. Stegelmann, N.C. Schiodt, C.T. Cambell, P. Stolze, J. Catal. 221 (2004) 630.
[36] M.D. Argyle, K. Chen, A.T. Bell, E. Iglesia, J. Catal. 208 (2002) 139.
[37] P. Dunn, H.G. Stenger Jr., I.E. Wachs, Catal. Today 51 (1999) 301.
[38] J.C. Wu, P. Harriot, J. Catal. 39 (1975) 395.
[39] M. Jarjoui, B. Moravec, P.C. Granelle, S.J. Teichner, J. Chim. Phys. 75 (1978) 1061.
[40] E.A. Podgornov, I.P. Prosvirin, V.I. Bukhtiyarov, J. Mol. Catal. A: Chem. 158 (2000) 337.